HHS Public Access

Author manuscript

Adv Healthc Mater. Author manuscript; available in PMC 2019 September 01.

Published in final edited form as:

Adv Healthc Mater. 2018 September ; 7(17): e1800332. doi:10.1002/adhm.201800332.

Crosstalk between autophagy and apoptosis contributes to ZnO nanoparticles-induced human osteosarcoma cell death

Guanping He[1], **Yunlong Ma**[2], **Ye Zhu**[3], **Lei Yong**[1], **Xiao Liu**[1], **Peng Wang**[1], **Chen Liang**[1], **Chenlong Yang**[1], **Zhigang Zhao**[1], **Bao Hai**[1], **Xiaoyu Pan**[1], **Zhongjun Liu**[1], **Xiaoguang Liu**[1,*], and **Chuanbin Mao**[3,*]

[1]Department of Orthopedics, Peking University Third Hospital, No. 49, North Garden Street, Haidian District, Beijing 100191, China

[2]The Center for Pain Medicine, Peking University Third Hospital, No. 49, North Garden Street, Haidian District, Beijing 100191, China

[3]Department of Chemistry & Biochemistry, Stephenson Life Sciences Research Center, University of Oklahoma, Norman, Oklahoma 73019, USA

Abstract

Killing osteosarcoma cells by zinc oxide nanoparticles (ZnO NPs) and its underlying sub-cellular mechanism have never been studied. Here we find that the NPs induced crosstalk between apoptosis and autophagy, which lead to osteosarcoma cell death. Specifically, the NP uptake promotes autophagy by inducing accumulation of autophagosomes along with impairment of lysosomal functions. The autophagy further causes the uptaken NPs to release zinc ions by promoting their dissolution. These intracellular zinc ions, together with those that are originally released from the extracellular NPs and flowed into the cells, collectively target and damage mitochondria to produce reactive oxygen species (ROS). Then the ROS inhibit cell proliferation by arresting S phase and trigger apoptosis by extrinsic and intrinsic pathways, ultimately leading to cell death. More importantly, suppression of the early stage autophagy restores cell viability by abolishing apoptosis whereas blockade of the late stage autophagy inversely enhances apoptosis. In contrast, inhibition of apoptosis shows a limited ability to restore cell viability but obviously enhance autophagy. Notably, cell viability is strongly ameliorated by the combination of inhibitors for both the late stage autophagy and the apoptosis. These findings provide a mechanistic understanding of the NP-directed autophagy and apoptosis in osteosarcoma cells.

Keywords

zinc oxide nanoparticles; human osteosarcoma cells; apoptosis; autophagy; crosstalk

[*]Corresponding Author: xgliudoctor@163.com (Xiaoguang Liu); cbmao@ou.edu (Chuanbin Mao).

Conflicts of Interest

The authors declare no conflict of interest.

Data availability

The raw data required to reproduce these findings are available upon requests.

1. Introduction

Osteosarcoma commonly occurs in children and young adults. It is a primary bone tumor that is most prevalent, malignant, aggressive and metastatic [1]. The currently used chemotherapies suffer drug resistance and cause serious side effects [2]. Thus, there is a pressing need in developing novel therapies to overcome the drug resistance while avoiding side effects for osteosarcoma therapy. Recently, it has been verified that nanoparticles (NPs) could overcome the multidrug resistance of cancer cells as they can successfully bypass the pathways for traditional chemotherapeutic drugs to enter cells [3]. Among the NPs, metal oxide NPs have recently received attention because they could be uptaken by cancer cells to cause cytotoxicity [4].

Zinc oxide nanoparticles (ZnO NPs), an FDA-approved pharmaceutical agent, are widely used in drug formulations and cosmetics, due to their stability, biocompatibility and safety [5]. Recently, a growing number of studies have proved a promising anti-tumor activity of ZnO NPs on many human cancer cell lines with dramatically less toxic effect on normal cells [4a, 6]. However, the underlying regulatory mechanism by which the ZnO NPs caused cancer cell death are still obscure. Moreover, the effect of ZnO NPs on one specific cell type, human osteosarcoma cells, have never been investigated before.

Cell cycle is an important process involved in cell proliferation and mediated by cyclin-dependent kinases (CDKs) and their inhibitors [7]. Cancer cells are characteristic of imbalanced cell cycle regulation, which is related to cancer development and occurrence [8]. During several phases in the cell cycle, successful accomplishment of S transition is a pivotal factor for DNA replication and cell progression [9]. It has been reported that S-phase arrest is a target for cancer therapeutics and could be induced by many cytotoxic agents [6a, 10].

It is still unknown whether ZnO NPs can induce type I (apoptosis) or type II (autophagy) programmed death of osteosarcoma cells although they were reported to cause the death of other cells [10a, 11]. Apoptosis is a key factor involved in chemotherapeautic cancer treatment [12]. Autophagy begins with the formation of phagophore, followed by the insertion of LC3 protein into the phagophore membrane to engulf intracellular cargos. Consequently, a double-membrane structure, autophagosome, is formed. The autophagosomes and lysosomes are then fused together to form autolysosomes. In the autolysosomes, the engulfed intracellular cargos will be biodegraded and recycled. Autophagy may promote cell survival and suppress apoptosis. It may also contribute to cell death, either together with apoptosis or replacing defective apoptosis.

Rapid release of zinc ions in a solution, especially in an acidic pH, is a characteristics of ZnO NPs [13]. Although zinc is a necessary trace element in the body [14], excessive accumulation of the local concentration of zinc ions will lead to cellular zinc homeostasis and cause lysosome and mitochondria damage [15]. However, whether zinc ions released from NPs or NPs themselves are responsible for the cell death remains to be ambiguous.

Cancer cells present a relatively high metabolic activity and a disordered mitochondrial function compared to normal cells, and thus they bear an improved level of reactive oxygen

species (ROS) in comparison to normal cells. Hence, the cancer cells are more vulnerable to ROS accumulation [16]. Excessive ROS can induce apoptosis and autophagy [17]. The classical AKT/mTOR pathway is also reported to be involved in autophagy [17]. However, it is still unknown whether the AKT/mTOR pathway was activated and ROS were produced in ZnO NPs-treated osteosarcoma cells.

Here we demonstrated that ZnO NPs could suppress osteosarcoma cell proliferation by causing S phase arrest and induce cell death due to an induction of both apoptosis and autophagy. We also studied the upstream Akt/mTOR signaling pathways and the possible regulatory mechanisms of the crosstalk between apoptosis and autophagy. We further clarified that ZnO NPs-induced osteosarcoma cell death resulted from a high concentration of intercellular zinc ions but not from NPs. Simultaneously, it was verified that ZnO NPs could utilize autophagy to enhance zinc ion release from the uptaken ZnO NPs. The released zinc ions, combined with the inflow of zinc ions (derived from the extracellular zinc ions release from ZnO NPs), target and damage the mitochondria, which could contribute to excessive ROS generation to promote apoptosis, ultimately triggering osteosarcoma cell death. These findings suggest an important biomedical application of ZnO NPs and provide a novel sight for targeting osteosarcoma.

2. Results

2.1 Characterization and cellular uptake of ZnO NPs

Our TEM observed that the ZnO NPs had a size of ~50nm and were roughly spherical (Figure 1c), which was in accord with the description of this nanoparticles purchased from sigma(677450). To verify the cellular uptake of NPs, we used TEM to observe the cells treated with ZnO NPs, and confirmed that the NPs were internalized mainly via large intracellular cytoplasmic vacuoles (Figure 1b,c).

2.2 ZnO NPs exhibited a preferential effect on the osteosarcoma cell proliferation

The four human osteosarcoma cell lines (U-2OS, MG-63, Saos-2, and143B) and two types of normal cell lines (HUVEC and hFOB1.19) were separately allowed to interact with ZnO NPs of various concentrations for different times (Figure 2a). After 24 h, the ZnO NPs have a different IC_{50} value for different cancer cell lines, specifically, 13.84 μg/ml for 143B, 32.43 μg/ml for U-2OS, 18.13 μg/ml for Saos-2 cells, and 23.4 μg/ml for MG-63. The IC_{50} for treatment with ZnO NPs for 48 h was 12.48 μg/ml for 143B, 28.49 μg/ml for U-2OS, 14.69 μg/ml for Saos-2 cells, and 21.49 μg/ml for MG-63. Treatment with ZnO NPs showed fewer colonies in both U-2OS and Saos-2 cells than those in control groups (Figure 2b). Moreover, HUVEC and hFOB1.19 cells showed obvious stronger resistance to ZnO NPs than that of the four osteosarcoma cell lines (Figure 2d). These results indicated that ZnO NPs inhibited the proliferation of human osteosarcoma cells in a dose- and time-dependent manner and demonstrated less cytotoxic effect against normal cells, which were in line with previous studies[6b, 13].

2.3 ZnO NPs induced S phase arrest

Previous studies have verified that ZnO NPs could induce cell cycle arrest to inhibit cell proliferation[18]. To verify that ZnO NPs suppressed the proliferation of osteosarcoma cells through triggering cell cycle arrest, we evaluated the change in the cell cycle distribution after the cancer cells were subjected to ZnO NPs treatment. Fig. 2c showed that ZnO NPs caused S phase accumulation and correspondingly G0/G1 phase in both U-2OS and Saos-2 cells was decreased. To understand the reason behind this observation, we quantified the expressions of Cdc25C, Cyclin A2, CDK1, and CDK2. We found that these four proteins, for driving the S to G2/M phase transition in a cell cycle, were obviously decreased in response to the ZnO NP treatments (Figure 2e). Hence, S phase was arrested after ZnO NPs treatment by altering S phase-regulating proteins.

2.4 ZnO NPs induced cell apoptosis

To verify that apoptosis contributed to the osteosarcoma cell proliferation inhibition by ZnO NPs, we performed DAPI staining, flow cytometry, transmission electron microscopy (TEM) imaging, and western blotting assays. Figures 3a showed that DNA fragmentation and chromatin condensation occurred after the cancer cells were exposed to ZnO NPs. To determine the apoptotic proportion, annexin V-FITC/PI was employed to stain the NP-treated osteosarcoma cells. Both early and late apoptotic proportion were increased in response to treatment with ZnO NPs for 24 h when compared to the control group (Figure 3b). JC-1 fluorescent probe was also used to label the mitochondrial membrane. Fluorescent microscopy showed an obvious shift from red to green in the mitochondrial membrane after ZnO NPs treatment (Figure S1b), indicating a decrease of the mitochondrial membrane potential (MMP) following ZnO NPs treatment as quantified by flow cytometry (Figure 3c). Moreover, western blotting detected an upregulation of Bax/Bcl2 ratio and a translocation of Cytochrome c (cyt c) from the cytoplasm to mitochondria after ZnO NPs treatment (Figure 3d, e, f). Then, we investigated the expression of major related proteins in the extrinsic and intrinsic apoptosis pathways. As showed in Figure 3d and e, ZnO NPs markedly changed the level of one marker for the intrinsic pathway (caspase-9), two markers for the extrinsic pathway (Fas and caspase-8), and one marker for both intrinsic and extrinsic pathway (caspase-3). Furthermore, we also conducted a protein activity assay to detect the caspase-3 activity. The result exhibited that the activity of the enzyme (caspase-3) was enhanced with the increase of the amount of ZnO NPs for treating the cancer cells (Figure 3g). To further verify that apoptosis contributed to the ZnO NPs-induced death of the osteosarcoma cells, we studied the U-2OS cell viability when they were first pretreated using z-vad-fmk (an apoptosis inhibitor, i.e., a well-known pan caspase inhibitor) and then exposed to ZnO NPs. Unexpectedly, the cell viability was only partially restored with no more than 10% (Figure 3h) although apoptosis was successfully inhibited (Figure 3i), suggesting that other pathways may be involved in ZnO NPs-induced osteosarcoma cell death.

2.5 ZnO NPs triggered autophagy by enhancing autophagosomes formation and impaired lysosomal function

It was recently known that autophagy could also contribute to cell death [10a, 11f, 11g]. We observed that ZnO NPs enhanced the immunofluorescence intensity of LC3 (Figure 4a). Our

TEM results showed that numerous vacuoles in the cytoplasm (a sign of autophagy), along with chromatin condensation (a sign of apoptosis), were found after the osteosarcoma cells were treated with ZnO NPs for 1 day in comparison to the untreated cell group. A higher magnification TEM image clearly demonstrated that degraded cytoplasmic materials were engulfed into autophagic vacuoles (Figure 4b). AO-staining assay also revealed the accumulation of bright red acidic vesicles after ZnO NPs treatment by fluorescence microscopy (Figure S1a) and flow cytometry (Figure 4c). Meanwhile, western blot analysis demonstrated an upregulation of the LC3-II/LC3-I ratio in response to ZnO NPs treatment (Figure 3d). These data demonstrated that ZnO NPs induced autophagosomes accumulation.

Enhanced accumulation of autophagosomes could arise from either enhancement of autophagosomes formation or blockade of autolysosomes formation. In order to understand which is the case for ZnO NP-induced autophagosome accumulation, we quantified the LC3-I to LC3-II transition with or without the addition of chloroquine (CQ), an inhibitor for increasing the pH of the lysosomes and blocking the capability for the autophagosomes to fuse with lysosomes. In the presence of the CQ, the level of LC3-II only depended on the formation of autophagosomes and thus served as a marker for the autophagy induction. Using the Western blot assay, we found that treatment with ZnO NPs led to an elevation in the LC3-II/ LC3-I ratio regardless of the presence of CQ (Figure 3e). These results suggested that ZnO NPs indeed led to autophagosomes formation but still could not preclude a possibility that the formation of autolysosomes was blocked due to the lysosomal function disruption. To understand this, the autophagic degradation was monitored by measuring the expression of SQSTM1/p62, which is a protein substrate that can be specifically integrated into the autophagosomes and biodegraded in the autolysosomes). Its expression was increased in the NP-treated cells, and further increased when CQ was present (Figure 4f). Taken together, we could conclude that ZnO NPs not only induced the formation of autophagy by enhancing autophagosomes but also impaired lysosomal function in human osteosarcoma cells.

2.6 Involvement of Akt/mTOR pathway in ZnO NPs-triggered human osteosarcoma cell death

Inhibiting Akt/mTOR pathway is recognized as a common and important regulatory mechanism of autophagy [19]. Fig. 4a confirmed that decrease in the levels of both p-Akt and p-mTOR was significant when the cells were treated with ZnO NPs and p-S6 (a substrate for mTOR). However, rapamycin (an inhibitor of m-TOR) failed to enhance cell death (Fig. 5b). These results suggested that although Akt/mTOR signaling pathway was activated, it was not the rate-limiting upstream pathway during the ZnO NPs-induced osteosarcoma cell death.

2.7 The role of zinc ions in NPs-triggered human osteosarcoma cell death

2.7.1 Elevation of intracellular zinc ions sequestrated by the mitochondrion contributed to osteosarcoma cell death.—

Since zinc ions can become toxic to the cells [13, 15b], we further examined the concentration of intracellular zinc ions after ZnO NPs treatment by ICP-MS. The results revealed that zinc ions concentration is markedly elevated in both U-2OS and Saos-2 cells (Figure 6a). Interestingly, Saos-2 cells contained a higher

level of zinc ions than U-2OS, which may be the reason why Saos-2 cells were more susceptible to ZnO NPs (Figure 2a). Considering the relationship between mitochondrion and apoptosis, we then respectively detected the level of zinc ions in the mitochondrion and cytoplasm. Figure S3a showed that the level of zinc ions obviously increased both in mitochondrion and cytoplasm while the level in mitochondrion was much higher than that in cytoplasm, indicating that increased intracellular zinc ions might be sequestrated by mitochondrion. To verify whether the increasing concentration of zinc ions enhanced the cell death, ethylenediaminetetraacetic acid (EDTA), which could chelate zinc ions, was added 1 h before ZnO NPs treatment to chelate zinc ions in solution. The cell ability assay showed that pretreatment with EDTA could completely abolish ZnO NPs-induced cell death regardless of its effect on cell viability (Figure 6b). ICP-MS also confirmed that intracellular zinc ions concentration nearly decreased to a normal level (Figure 6h), indicating that ZnO NPs-induced cell death was due to the elevation of the level of intracellular zinc ions. To further verify this hypothesis, we evaluated the effect of the $ZnCl_2$ solution. The result showed that $ZnCl_2$ solution could also induce cell death in a way similar to ZnO NPs and successfully induce autophagy and apoptosis, as evidenced by upregulating the expression of related proteins (Figure 6c,d). To further investigate whether the high concentration of intracellular zinc ions was the sole mediator contributing to the cell death, we compared the concentration of intercellular zinc ions under the equivalent inhibitory effect of $ZnCl_2$ and ZnO NPs solution. The data exhibited that the level of zinc ions in ZnO NPs group was even higher than the $ZnCl_2$ group (Figure 6e), suggesting that the intracellular zinc ion concentration treated with ZnO NPs possessed the ability to kill the human osteosarcoma cells alone. In addition, our TEM directly showed that the cell ultrastructure was nearly intact after pretreatment with EDTA regardless of uptaken ZnO NPs (Figure 5b), indicating that it was the intracellular zinc ions but not NPs that contributed to the cell death. Collectively, these results confirmed that high concentration of intracellular zinc ions was the source of inducing human osteosarcoma cell death.

2.7.2 Intracellular zinc ions inflowed from extracellular source and released from uptaken NPs synergistically led to NPs-induced human osteosarcoma cell death.—After we had proved that zinc ions triggered the osteosarcoma cell death, efforts were made to clarify whether the cell death resulted from the inflowed zinc ions uptaken from the extracellular environment or those released from the uptaken ZnO NPs, or a combination of both. Thus, $CaCl_2$ solution, a common agent to block zinc ions uptake[20], was used to evaluate whether zinc ions uptake was required for ZnO NPs-induced cell death. Our data showed that CaCl2 treatment could completely abolish ZnO NPs-induced cell death (Figure 6f). Additionally, the ICP-MS confirmed that the level of zinc ions in the supernatant was increased while the amount of intracellular zinc ions was correspondingly reduced (Figure 6g, h). These data suggested that CaCl2 successfully impeded the entry of toxic zinc ions into the cells and then prevented cell death. Unexpectedly, western blot results from the cells pretreated with CaCl2 showed a considerably higher LC3-II/LC3-I ratio than the EDTA and control groups, but all of those groups did not detect the cleavage of pro-caspase3 (Figure 6i), indicating that the level of intracellular zinc ions with the addition of CaCl2 was not high enough to cause cell death but have the ability to induce autophagy. Our TEM results clearly exhibited cell ultrastructure without obvious damage but

with obvious accumulation of autophagic vacuoles (Figure S2b), which were in accordance with the result of western blotting. These data suggested that the zinc ions, which were released from the extracellular ZnO NPs and then flowed into the cells, as well as intracellular zinc ions, which were released from the uptaken ZnO NPs, were both important for ZnO NPs-induced cell death. To test this hypothesis, we quantified the concentration of zinc ions in the DMEM medium after the ZnO NPs were placed in the medium. A standard filter assay revealed that the released zinc ion concentration in DMEM was elevated from 0.34 to 24.4 μg/mL after the NPs were incubated in the medium for one day at the body temperature (Figure 6g). Zinc ions at these concentrations were not toxic to the osteosarcoma cells according to the inhibitory curve of $ZnCl_2$ (Figure 6c). Even when the concentration of $ZnCl_2$ reached 50 μg/ml, approximately twice that of released zinc ions from ZnO NPs, the zinc ions still did not show high cell viability inhibition (Figure 6c). These data suggested that the inflow of extracellularly released zinc ions was an indispensable but not the sole determining factor in ZnO NPs-induced cell death. Taken together, we could come to a conclusion that the inflow of the extracellularly released zinc ions (from extracellular ZnO NPs) and production of intracellular released zinc ions (from uptaken ZnO NPs) synergistically led to human osteosarcoma cell death.

2.8 Crosstalk between apoptosis and autophagy in ZnO NPs-induced human osteosarcoma cell death

Apoptosis can be interrelated to autophagy [21]. However, the crosstalk between them in ZnO NPs-induced death of cancer cells has never been explored. To fill this gap, first, we examined the effect of apoptosis suppression on the autophagy. Figures 7a showed that z-vad-fmk significantly enhanced the level of AO-staining. Correspondingly, western blotting revealed that the LC3-II/ LC3-I ratio was further increased in the presence of the apoptosis inhibitor in comparison to the control group without cleavage of pro caspase-3 (Figure 7b), suggesting that the mechanism of cell death was changed from apoptosis to autophagy when the inhibitor was used to inhibit apoptosis. These results indicated that inhibiting apoptosis would enhance autophagy. Next, we examined the apoptosis when the autophagy was suppressed by an inhibitor. Autophagy included the phase of forming autophagosomes (at the early stage of autophagy) and another phase of forming autolysosomes (at the late stage of autophagy) [21]. Here we respectively blocked these two phases to observe the influence on ZnO NPs-triggered human osteosarcoma cell death. We found that 3-MA, an inhibitor for inhibiting the autophagosomes formation, prevented the ZnO NPs-induced cell death regardless of the influence of the inhibitor itself (Figure 7c). The flow cytometry revealed that 3-MA sharply decreased the proportion of AO-staining approximately to a normal level (Figure 6d), and completely avoided the NP-induced apoptosis (Figure 7d) and MMP reduction (Figure S3a). This was further evidenced by inhibiting the LC3-II/ LC3-I ratio and diminishing the procaspase-3 cleavage (Figure 7e). Moreover, 3-MA also reduced the concentration of intracellular zinc ions (Figure 7i). These results revealed that autophagosomes induction was positively related to the elevating concentration of intracellular zinc ions and ZnO NPs-induced cell death. Then, we blocked the late stage of autophagy (autolysosomes formation) with CQ, the result unexpectedly showed that CQ not only failed to rescue the fate of cell death but inversely promote the apoptosis without a significant fluctuation of intracellular zinc ion concentration (Figure 7f, g, h), suggesting

that the cells could shift to the status of apoptosis when autolysosomes formation was blocked, and this process seemed not related with the concentration of intracellular zinc ions. To further verify whether there really existed a conversion between the late stage of autophagy and apoptosis, cell viability assay was analyzed in the cells co-treated with ZnO NPs and CQ combined with z-vad-fmk. As we expected, the result showed a considerable increase of the cell viability (Figure 7j), indicating that there indeed existed a conversion between autophagy and apoptosis. Collectively, we could conclude that inhibiting the autophagosomes formation could downregulate the level of intracellular zinc ions and then abolish ZnO NPs-induced osteosarcoma cell death while suppression of either the formation of autolysosomes or apoptosis would push one to the other.

2.9 ZnO NPs induced ROS generation contributed to ZnO NPs-induced human osteosarcoma cell death.

2.9.1 ROS generation triggered apoptosis and S phase arrest—ROS could regulate cell cycle arrest and apoptosis[22]. Figure 8a showed that ROS level was higher in both low and high concentrations at 24 h than the control groups. Interestingly, the high concentration group contained a relatively lower level of ROS production compared to the low concentration group, probably because the high concentration would lead to severe cell damage, resulting in the leak of ROS production. We further used an ROS scavenger (NAC) to verify that ROS were involved in ZnO NPs-triggered cell death. We found that NAC inhibited the ROS production triggered by ZnO NPs (Figure S3b), avoiding NP-induced apoptosis (Figure 8b, c) and MMP reduction (Figure S3c). In addition, NAC also inhibited ZnO NP-induced S phase arrest and the change in the regulator markers of the S cell cycle (Figures 8d. e). All these data revealed that ROS was the upstream of apoptosis and S phase arrest in ZnO NPs-induced osteosarcoma cell death.

2.9.2 Co-promotion between autophagy and ROS—ROS induced by different kinds of NPs have been reported to be the upstream of autophagy [23]. Thus, we considered whether ZnO NPs-induced ROS were the autophagy inducer. To determine the influence of ROS generation on the ZnO-NPs-induced autophagy, we quantified the AO-staining intensity and LC3-II/LC3-I ratio with and without the addition of NAC. Figure 8f, h showed that NAC clearly decreased the LC3-II/LC3-I ratio when ZnO NPs were present and obviously weakened the AO-staining intensity. In contrast, Figure 8g revealed that 3-MA could also reduce the ROS level. These results suggested that there might exist a co-promotion relationship between the autophagy and ROS.

3. Discussion

Recently, it has been demonstrated that ZnO NPs contain an antitumor potential with a higher cancer cell selectivity compared to the traditional chemotherapeutic agents [13]. However, the mechanism at the sub-cellular level has never been deeply studied before [6a, 10a, 11g]. Moreover, no study has been made about the ZnO NPs induced osteosarcoma cell death. In this work, by systematically studying the role of autophagy and apoptosis as well as their crosstalk in inducing the death of ZnO NPs-treated cells, and the role of zinc

ions in the apoptosis and autophagy, we have made a step further to the understanding of the sub-cellular mechanism by which ZnO NPs triggered cancer cell death.

We discovered that the apoptosis of osteosarcoma cells was triggered by ZnO NPs through activating the extrinsic and intrinsic pathways (Figure 3d,e,f). However, the caspase inhibitor z-vad-fmk only partially prevented the cell death, suggesting that there might exist other caspase-independent pathways in ZnO NP-induced human osteosarcoma cell death (Figure 3h,i). In our study, autophagy was induced and confirmed by the formation of autophagosomes, enrichment of acidic vesicles (AO-staining), enhancement of LC3 immunofluorescence and up-regulation of LC3-II/ LC3-I ratio (Figure 4a, b, c, d). It was further confirmed by the elevation of the LC3-II/ LC3-I ratio when the autolysosomes formation was blocked (Figure 4e). Moreover, we found that ZnO NPs treatment elevated the level of p62 expression, suggesting that autophagic flux was impaired by ZnO NPs treatment (Figure 4f). Autophagy can be negatively regulated by Akt/mTOR signaling through mediating the phosphorylation of mTOR [17]. Our current results showed that ZnO NPs triggered inhibition of p-Akt, p-mTOR and p-S6 (Figure 5a). However, suppression of m-TOR with rapamycin failed to promote osteosarcoma cell death (Figure 5b), suggesting that Akt/m-TOR signaling pathway might be involved in but not the determining upstream pathway for autophagy. Further work is needed to clarify which upstream pathway is the dominant factor in triggering autophagy.

Our data also confirmed an obvious increase in the level of intracellular zinc ions in cytosol and mitochondria. We further observed a tendency that the concentration of zinc ions in mitochondria was much higher than that in cytosol, indicating that zinc ions uptake into cytosol would be eventually sequestrated by mitochondria (Figure S2a). Furthermore, we confirmed that it was the zinc ions but not the NPs that actually contributed to the human osteosarcoma cell death by comparing the concentration of intracellular zinc ions after ZnO NPs and $ZnCl_2$ solution treatment under the condition of the equivalent killing effect. We further verified that the cell death was completely abolished by zinc-specific chelating agents such as EDTA (Figure 6b). We also provided that both the inflow of extracellularly released zinc ions (from extracellular ZnO NPs) and the intracellular released zinc ions (from uptaken ZnO NPs) were indispensable for ZnO NPs-induced human osteosarcoma cell death.

From the above experimental results, we proposed a new mechanism of ZnO NPs induced osteosarcoma cell death. Namely, our work showed that ZnO NPs induced osteosarcoma cell death through the crosstalk between two mechanisms of programmed cell deaths, the autophagy and apoptosis (Fig. 9). Specifically, the uptake of ZnO NPs induced the accumulation of autophagosomes and impaired the lysosomal functions, promoting the early and late stage of autophagy, respectively. The autophagy further triggered the zinc ions release from the uptaken ZnO NPs. The resultant zinc ions, together with the inflowed zinc ions (released from the extracellular ZnO NPs), collectively targeted and damaged the mitochondria, resulting in the generation of ROS. The ROS then inhibited the cell proliferation by S phase arrest and induced cell apoptosis through the extrinsic and intrinsic pathways, ultimately leading to cell death. This crosstalk mechanism has been further supported by three important results. First, the elimination of ROS with NAC completely

reversed the cell viability (Fig. 8b). Second, inhibiting the early stage of autophagy with 3-MA abolished the apoptosis while inhibiting the late stage of autophagy with CQ inversely promoted the apoptosis (Fig. 7e, g). Third, suppressing apoptosis with z-vad-fmk failed to rescue cell death but enhanced autophagy (Fig. 7a, b).

4. Conclusion

In conclusion, our study provided potential mechanistic pathways for ZnO NPs-induced human osteosarcoma cell death. We discovered that ZnO NPs could suppress the proliferation of human osteosarcoma cells through the induction of S phase arrest and trigger the cell death through mediating autophagy and apoptosis in a ROS-dependent manner. We also clarified that apoptosis inhibition would contribute to autophagy whereas suppressing the early or late stage of autophagy resulted in an inverse effect on the cell death. In addition, we determined that it was the intracellular zinc ions but not the NPs themselves that initiated the process of the cell death, and ZnO NPs could induce autophagy to regulate zinc ions releasing. Collectively, the ZnO NPs-induced cross-talk between the autophagy and apoptosis determined the cell fate. These compelling results expanded our understanding of clinical applications of ZnO NPs for targeted osteosarcoma therapy.

5. Materials and Methods

5.1 Reagents, antibodies, nanoparticles and cells

All chemicals, including Acridine Orange dye (AO), chloroquine (CQ), Ethylenediaminetetraacetic acid (EDTA), z-vad-fmk, N-Acetyl-L-cysteine (NAC), JC-1 dye, $CaCl_2$, 3-Methyladenine (3-MA), and Rapamycin, were purchased and directly used without any further purification. Ultrapure water (Milli-Q Biocel) was used as universal solvent unless otherwise indicated. Antibodies against Bax, Bcl-2, Fas, LC3, SQSTM1/p62, AKT, m-TOR, S6, CDK1, CDK2, CDC25C, Cyclin A2, caspase-9, caspase-8, caspase-3, Cytochrome c, β-actin and GAPDH were also used as received. ZnO NPs were obtained from Sigma-Aldrich(677450). Their shape and size were confirmed by TEM. All cells used were purchased from ATCC, including four human osteosarcoma cell lines (U-2OS, MG-63, Saos-2, 143B).

5.2 Exposure of cells to nanoparticles

ZnO NPs were placed in ultrapure water to form a suspension of 1 mg/ml and immediately dispersed under sonication (200 W for 30 min) to make the suspension fully dispersed. Then the suspensions were added into the complete medium to give final concentrations, which range from low to high dose (5, 10, 20, 30, 40, 50 μg/ml). Finally, the NPs were placed into the cell culture medium at varying concentrations.

5.3 Cell viability assay

CCK-8 kit, from Dojindo Laboratories (Kumamoto, Japan), was utilized to characterize the inhibition of cell proliferation by ZnO NPs following a reported protocol [24]. Cell culture medium without NPs or with NPs alone (No cells) was also characterized as controls. In the

rescue experiments, the cells were first treated with EDTA, $CaCl_2$, NAC, 3-MA, z-vad-fmk, and CQ for about 1 h.

5.4 Colony formation assay

Cells with a seeding density of 100 cells/well were cultured. After the overnight, they were co-cultured with ZnO NPs at varying concentrations for about 10 days till colonies were visible. 4% paraformaldehyde was used to fix the colonies and then 0.1% crystal violet was used to stain them for 10 min. Finally, the visible colonies were counted.

5.5 DAPI staining

The changes of apoptotic characteristic were assessed by DAPI staining. After staining, a fluorescence microscope was used to visualize the chromatin condensation as well as nuclei fragmentation.

5.6 TEM imaging

NPs-induced change in the cell ultrastructure was observed by TEM. Apoptosis and autophagy were determined by observing cell nuclear condensation and autophagosomes formation. Briefly, the cells were purified by centrifugation (800g) after tyrosination and then successively fixed first by 2.5% glutaraldehyde and by 1% osmium tetroxide, and then treated with alcohol for dehydration. Finally, the cell pellets were placed into epoxy by embedding. Ultrathin sections were obtained using a microtome and observed under TEM.

5.7 FACS analysis

Cells with a seeding density of 2×10^5 cells per well were interacted with ZnO NPs of varying concentrations for one day. To determine NPs-triggered change in cell cycle, the cells were purified by centrifugation after treatment treated with ZnO NPs, then treated with 70% ethanol in a freezer (−20 °C). They were then incubated with PI/RNase staining buffer at 37 ℃ for half an hour. To detect apoptosis, the cells were labeled using Annexin V-FITC/Propidium Iodide Apoptosis Detection Kit for 15 min under no light condition. Then the cells were purified and then resuspended in PBS. An ROS Assay kit with DCFH-DA was utilized to verify ROS production. A JC-1 fluorescent probe was used to quantifying the MMP changes. For detecting the function of lysosomes, an acridine orange (AO) dye was diluted in complete medium to 1 μM, then incubated with cells at 37 °C for half an hour. The cells stained as above were then quantified by a flow cytometer.

5.8 Caspase-3 activity assay

A Caspase Activity Kit was purchased from Beyontime Biotechnologies in China and used to quantify the activity of the enzyme Caspase-3. After the NPs were interacted with the cells for one day, the cell lysates were prepared, and the enzymatic activity was measured following the manufacturer's protocol and reflected as the absorbance of the enzyme substrate at 405 nm.

5.9 Zinc ion release assay

ZnO NPs suspension (1 mg/ml, diluted with ultrapure water) was added into DMEM complete culture medium to reach a mixture concentration (50 μg/mL). The cells were then incubated for one day and ultracentrifuged (15000 g for 30 min) to detach the NPs. Then, HNO3 and H2O2 were used to dissolve the resulting supernatant. Finally, the concentration of zinc ions in the resultant solution was determined using inductively coupled plasma-mass spectrometry (ICP-MS). To detect the total intercellular zinc ion concentrations, the cells were allowed to interact with 50 μg/mL NPs with or without being pretreated with EDTA, $CaCl_2$, 3-MA, CQ or $ZnCl_2$ (100 μg/mL) for one day. Then the cells were washed and collected, then divided into two groups. One group was used to measure protein content, and the other was used to quantify the zinc ions by ICP-MS. To separately quantify the concentration of zinc ions in cytoplasm and mitochondria after ZnO NPs-treated cells. Fractions of cytoplasm and mitochondria were separated by Cell Mitochondria Isolation Kit (Beyotime Biotechnology, Jiangsu, China) and then divided into two tubes followed as above.

5.10 Immunofluorescence microscopy

After the cells with an original seeding density of 5×105/well were interacted with ZnO NPs for 24 h, they were then fixed with 4 % paraformaldehyde followed by one-hour treatment with 5% BSA to achieve blocking. Thereafter, the cells were stained first with an anti-LC3 antibody for one hour and then with a Cy™3 488-conjugated AffiniPure goat anti-rabbit IgG for one hour, followed by DAPI staining and fluorescence microscopy imaging.

5. 11 Western blot analysis

The cells were first interacted with ZnO NPs for one day. Then they were collected and lysed using RIPA lysis buffer added with protease and phosphatase inhibitors. Ultracentrifugation was carried out to purify the lysates and the resultant supernatant was treated using a mitochondria isolation kit in order to evaluate the changes of cytochrome c in the sub-cellular location, extracts of cytosolic, and mitochondrion. After the corresponding proteins were purified, their concentrations were quantified by a BCA protein assay kit. The fluorescent bands on the membranes stained with fluorescent antibodies were quantified by grave value analysis with respect to a control protein.

5.12 Statistical analysis

The data were all presented as means ± standard deviation. The statistical differences between experimental groups were analyzed by Graphpad Prism 6 using the paired Dunnett`s t-test or one-way ANOVA with a 95% con dence interval. A comparison under *, #P<0.05 is considered statistically different between two groups.

Supplementary Material

Refer to Web version on PubMed Central for supplementary material.

Acknowledgments

This work was financially aided by the National Natural Science Foundation of China (NO.81472041). We feel grateful to the Medical Research Center of Peking University Third Hospital for providing technical support. YZ and CM would also like to thank the financial support from National Institutes of Health (CA200504, CA195607, and EB021339).

References

[1]. a) Raymond AK, Jaffe N, Cancer Treat Res 2009, 152, 63; [PubMed: 20213386] b) Arndt CA, Rose PS, Folpe AL, Laack NN, Mayo Clin Proc 2012, 87, 475. [PubMed: 22560526]

[2]. a) Vos HI, Coenen MJ, Guchelaar HJ, Te Loo DM, Drug Discov Today 2016, 21, 1775; [PubMed: 27352631] b) Yan GN, Lv YF, Guo QN, Cancer Lett 2016, 370, 268; [PubMed: 26571463] c) Gill J, Ahluwalia MK, Geller D, Gorlick R, Pharmacol Ther 2013, 137, 89. [PubMed: 22983152]

[3]. Li B, Xu H, Li Z, Yao M, Xie M, Shen H, Shen S, Wang X, Jin Y, Int J Nanomed 2012, 7, 187.

[4]. a) Rasmussen JW, Martinez E, Louka P, Wingett DG, Expert Opin Drug Deliv 2010, 7, 1063; [PubMed: 20716019] b) Chakraborti S, Chatterjee T, Joshi P, Poddar A, Bhattacharyya B, Singh SP, Gupta V, Chakrabarti P, Langmuir 2010, 26, 3506. [PubMed: 20000758]

[5]. Zhang Y, Nayak TR, Hong H, Cai W, Curr Mol Med 2013, 13, 1633. [PubMed: 24206130]

[6]. a) Sirelkhatim A, Mahmud S, Seeni A, Kaus NHM, J Nanopart Res 2016, 18;b) Hanley C, Layne J, Punnoose A, Reddy KM, Coombs I, Coombs A, Feris K, Wingett D, Nanotechnology 2008, 19, 295103; [PubMed: 18836572] c) Franklin RB, Costello LC, J Cell Biochem 2009, 106, 750. [PubMed: 19160419]

[7]. Ingham M, Schwartz GK, J Clin Oncol 2017, 35, 2949. [PubMed: 28580868]

[8]. a) Stewart ZA, Westfall MD, Pietenpol JA, Trends Pharmacol Sci 2003, 24, 139; [PubMed: 12628359] b) Schwartz GK, Shah MA, J Clin Oncol 2005, 23, 9408. [PubMed: 16361640]

[9]. Dickson MA, Schwartz GK, Curr Oncol 2009, 16, 36.

[10]. a) Arakha M, Roy J, Nayak PS, Mallick B, Jha S, Free Radic Biol Med 2017, 110, 42; [PubMed: 28528796] b) Xu Z, Zhang F, Bai C, Yao C, Zhong H, Zou C, Chen X, J Exp Clin Cancer Res 2017, 36, 124. [PubMed: 28893319]

[11]. a) Wahab R, Siddiqui MA, Saquib Q, Dwivedi S, Ahmad J, Musarrat J, Al-Khedhairy AA, Shin HS, Colloids Surf B Biointerfaces 2014, 117, 267–276; [PubMed: 24657613] b) Daniel AG, Peterson EJ, Farrell NP, Angew Chem Int Ed 2014, 53, 4098;c) Ng KW, Khoo SP, Heng BC, Setyawati MI, Tan EC, Zhao X, Xiong S, Fang W, Leong DT, Loo JS, Biomaterials 2011, 32, 8218; [PubMed: 21807406] d) Ahamed M, Akhtar MJ, Raja M, Ahmad I, Siddiqui MK, AlSalhi MS, Alrokayan SA, Nanomedicine 2011, 7, 904; [PubMed: 21664489] e) Kleinsasser, Int J Oncol 2010, 37;f) Zhang J, Qin X, Wang B, Xu G, Qin Z, Wang J, Wu L, Ju X, Bose DD, Qiu F, Zhou H, Zou Z, Cell Death Dis 2017, 8, e2954; [PubMed: 28749469] g) Bai DP, Zhang XF, Zhang GL, Huang YF, Gurunathan S, Int J Nanomed 2017, 12, 6521.

[12]. Zimmermann KC, Bonzon C, Green DR, Pharmacol Ther 2001, 92, 57. [PubMed: 11750036]

[13]. Sasidharan A, Chandran P, Menon D, Raman S, Nair S, Koyakutty M, Nanoscale 2011, 3, 3657. [PubMed: 21826307]

[14]. a) Prasad AS, Mol Med 2008, 14, 353; [PubMed: 18385818] b) Vallee BL, Auld DS, Biochemistry 1990, 29, 5647. [PubMed: 2200508]

[15]. a) Shen C, James SA, de Jonge MD, Turney TW, Wright PF, Feltis BN, Toxicol Sci 2013, 136, 120; [PubMed: 23997113] b) Johnson BM, Fraietta JA, Gracias DT, Hope JL, Stairiker CJ, Patel PR, Mueller YM, McHugh MD, Jablonowski LJ, Wheatley MA, Katsikis PD, Nanotoxicology 2015, 9, 737; [PubMed: 25378273] c) Cho WS, Duffin R, Howie SE, Scotton CJ, Wallace WA, Macnee W, Bradley M, Megson IL, Donaldson K, Part Fibre Toxicol 2011, 8, 27. [PubMed: 21896169]

[16]. a) Kawagishi H, Finkel T, Nat Med 2014, 20, 711; [PubMed: 24999942] b) Vander Heiden MG, Cantley LC, Thompson CB, Science 2009, 324, 1029. [PubMed: 19460998]

[17]. Levy JMM, Towers CG, Thorburn A, Nat Rev Cancer 2017, 17, 528. [PubMed: 28751651]

[18]. a) Chan CF, Lan RF, Tsang MK, Zhou D, Lear S, Chan WL, Cobb SL, Wong WK, Hao JH, Wong WT, Wong KL, J Mater Chem B 2015, 3, 2624;b) Li H, Chadbourne FL, Lan R, Chan CF, Chan WL, Law GL, Lee CS, Cobb SL, Wong KL, Dalton Trans 2013, 42, 13495; [PubMed: 23897392] c) Chan CF, Tsang MK, Li HG, Lan RF, Chadbourne FL, Chan WL, Law GL, Cobb SL, Hao JH, Wong WT, Wong KL, J Mater Chem B 2014, 2, 84.

[19]. a) Zhu L, Guo D, Sun L, Huang Z, Zhang X, Ma W, Wu J, Xiao L, Zhao Y, Gu N, Nanoscale 2017, 9, 5489; [PubMed: 28401217] b) Roy R, Singh SK, Chauhan LK, Das M, Tripathi A, Dwivedi PD, Toxicol Lett 2014, 227, 29. [PubMed: 24614525]

[20]. He J, Xiao S, Wu Z, Yuan Z, Eur Spine J 2016, 25, 1373. [PubMed: 27001138]

[21]. Maiuri MC, Zalckvar E, Kimchi A, Kroemer G, Nat Rev Mol Cell Biol 2007, 8, 741. [PubMed: 17717517]

[22]. Ghavami S, Eshragi M, Ande SR, Chazin WJ, Klonisch T, Halayko AJ, McNeill KD, Hashemi M, Kerkhoff C, Los M, Cell Res 2010, 20, 314. [PubMed: 19935772]

[23]. a) Khan MI, Mohammad A, Patil G, Naqvi SA, Chauhan LK, Ahmad I, Biomaterials 2012, 33, 1477; [PubMed: 22098780] b) Li JJ, Hartono D, Ong CN, Bay BH, Yung LY, Biomaterials 2010, 31, 5996. [PubMed: 20466420]

[24]. Hao L, Yang H, Du C, Fu X, Zhao N, Xu S, Cui F, Mao C, Wang Y, J Mater Chem B 2014, 2, 4794. [PubMed: 25328680]

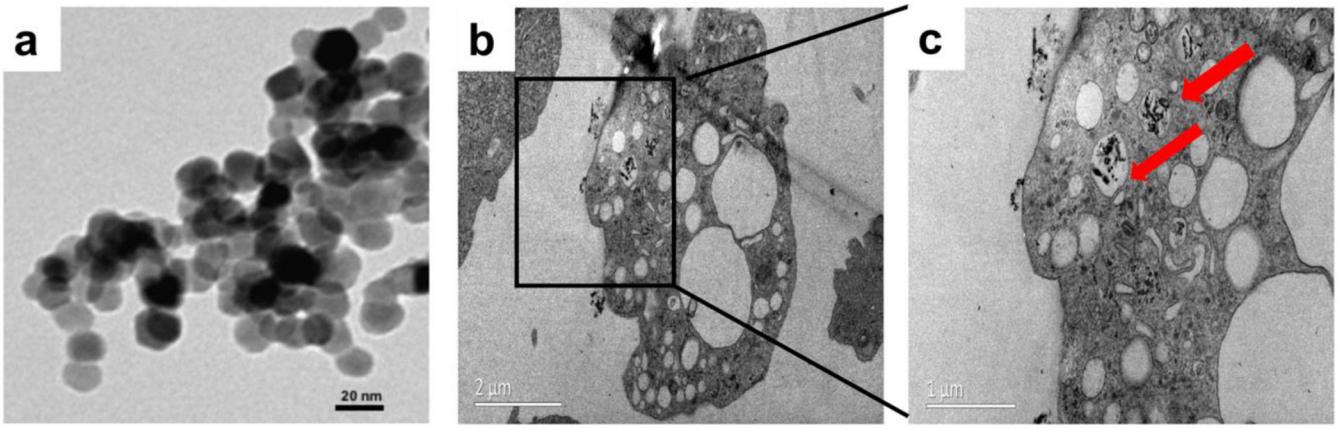

Figure 1.

Physical properties and uptake of ZnO NPs. (a) Transmission electron micrograph (TEM) showed that ZnO NPs were mainly spherical. Scale bar: 20 nm. (b,c) TEM images of U-2OS cells treated with 50 μg/ml ZnO NPs for 24 h. Red arrows indicated that ZnO NPs were wrapped into cells, Bar(b):2 μm, Bar(c): 1 μm.

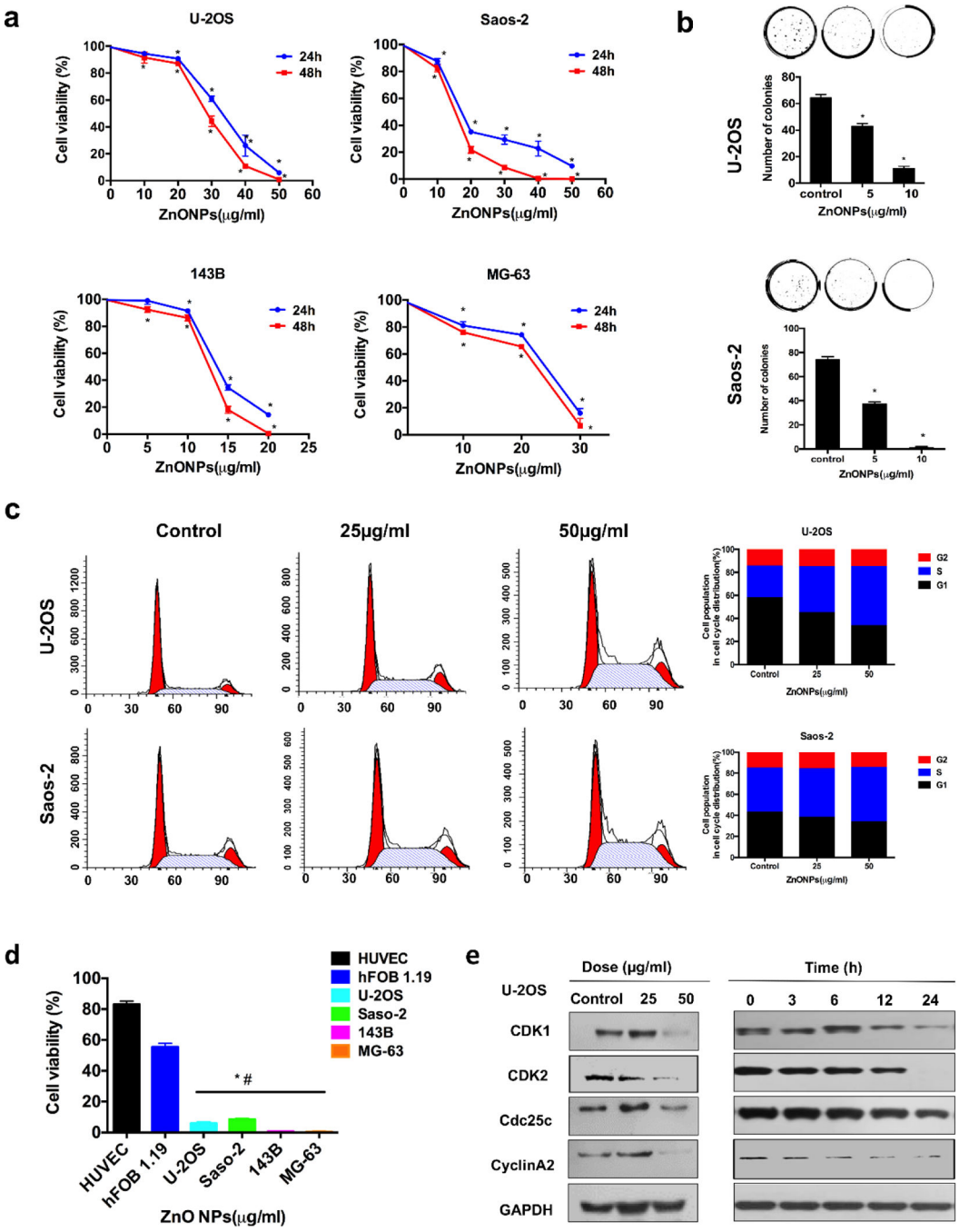

Figure 2.

Cell proliferation inhibition and S phase arrest induced by ZnO NPs in osteosarcoma cells. (a) The anti-proliferative effect of ZnO NPs on four osteosarcoma cells determined by a CCK-8 assay for a period of 24 and 48 h. (b) Colony formation assay of U-2OS and Saos-2 cells exposed to ZnO NPs. (c) Flow cytometry analysis of the cell cycle after the cells were exposed to ZnO NPs for 24 h. (d) Comparison of the inhibitory effect on four osteosarcoma cell lines and two normal cell lines by ZnO NPs (50 μg/ml) for 24h. (e) Western blot analysis of the cell cycle-regulated proteins expressions in the U-2OS cells after they were

treated with ZnO NPs of varying concentrations for 24 h or with ZnO NPs (50 μg/ml) for different times. Statistically significant differences were evaluated using the paired Dunnett`s t-test or one-way ANOVA. Results were expressed as the mean ± S.D. from three independent experiments. *P<0.05 versus control.

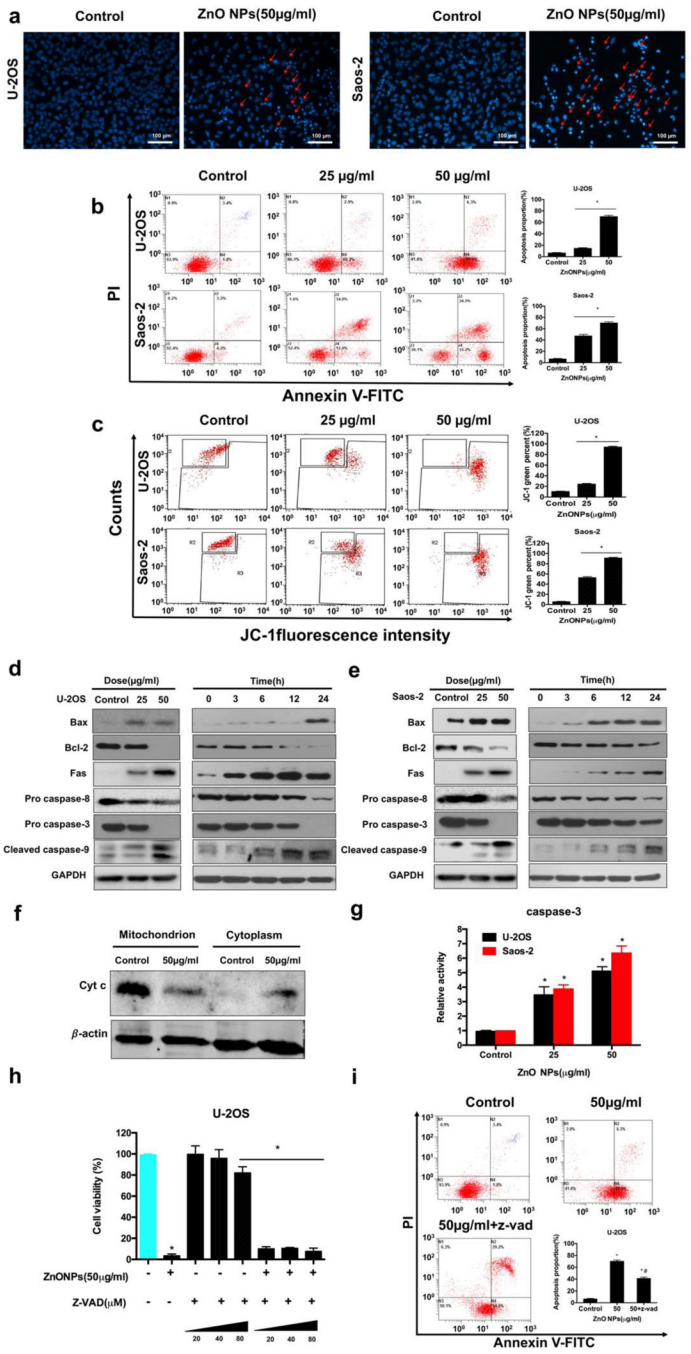

Figure 3.

Apoptosis induced by ZnO NPs in osteosarcoma cells. (a, b, c) Apoptotic morphological changes (×200) (a) as well as the flow cytometry of apoptotic proportion (b) and MMP (c) after the cells were treated with ZnO NPs (50 μg/ml) for 24 h. Apoptotic morphological changes were observed by fluorescent microscopy with DAPI staining. Red arrows indicated DNA fragmentation and chromatin condensation (×400). Cells were stained with annexin V-FITC/PI and apoptotic proportion was quantified by flow cytometry. The MMP stained with the JC-1 fluorescent probe was assessed by flow cytometry. (d, e, f) Western blot analysis

after the cells (d, U-2OS; e, Saos-2) were treated with various concentrations of ZnO NPs for 24 h (left panel) or incubated with ZnO NPs (50 μg/ml) for different times (right panel of d and e, and f). The expressions of Bax, Bcl-2, Fas, pro capsase-8, cleaved caspase-9 and pro capase-3 were determined by western blot (d and e). The expression of Cytochrome c (Cyt c) in cytoplasm and mitochondrion was respectively detected by western blot exposed to ZnO NPs (50 μg/ml) for 24 h (f). (g) Caspase-3 activity of the cells after the cells were treated with various concentrations of ZnO NPs for 24 h. (h) The cell viability treated with ZnO NPs (50 μg/ml) for 24 h was detected by the CCK-8 assay after the cells were pretreated with a caspase inhibitor, z-vad-fmk, with varying concentrations for 2 h. (i) Apoptosis stained with annexin V-FITC/PI was analyzed by flow cytometry with and without the addition of z-vad-fmk (20 μM). Statistically significant differences were evaluated using the paired Dunnett`s t-test or one-way ANOVA. Results were expressed as the mean ± S.D. from three independent experiments. *$P<0.05$ versus control.

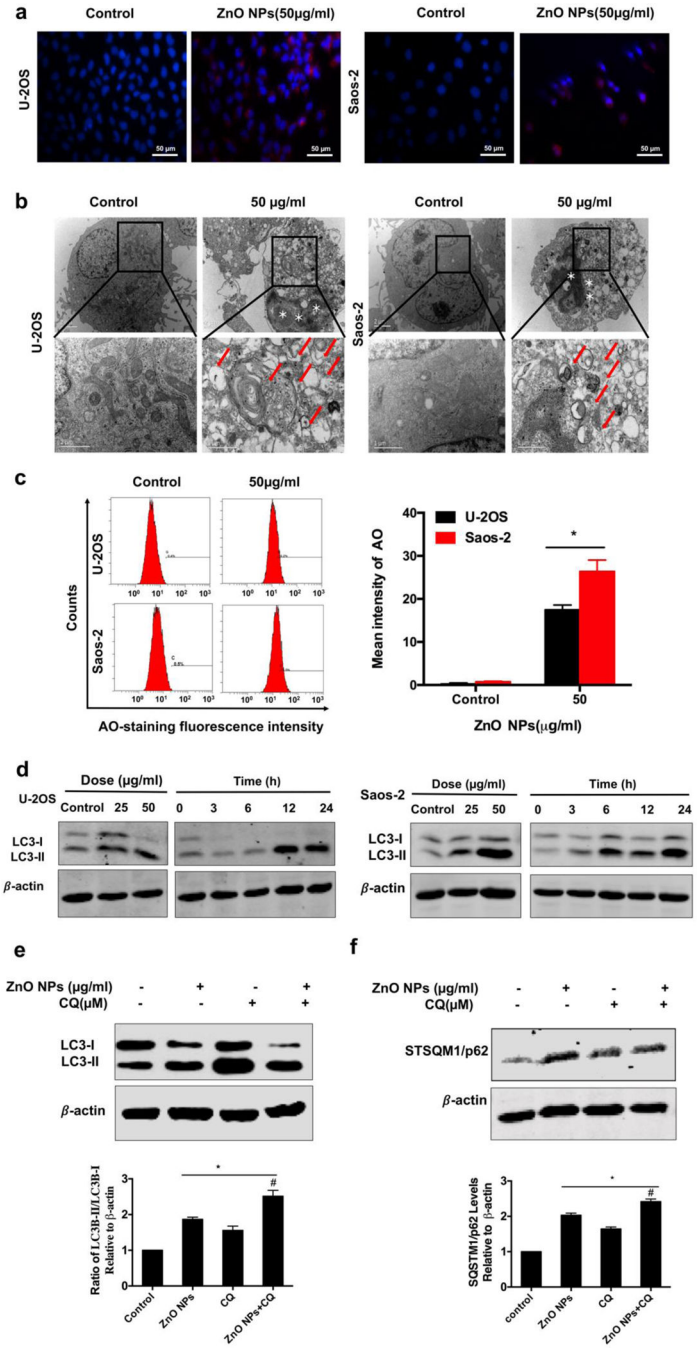

Figure 4.

Autophagy involved in ZnO NPs-induced osteosarcoma cell death with impairment of lysosomal functions. (a) Immunofluorescence staining of the LC3 protein in U-2OS and Saos-2 treated with 50 μg/ml ZnO NPs for 24 h (×400). (b) TEM images showing the formation of autophagosomes and ultrastructural change of nucleus. Red arrows indicated autophagosomes containing intact and degraded cellular debris. Asterisks indicated nuclear condensation or fragmentation. (c) Flow cytometry of the cells after they were treated with or without ZnO NPs for 24 h and stained with AO. (d) Western blotting analysis of LC3

levels after the cells were treated with various concentrations of ZnO NPs for 24 h or incubated with ZnO NPs (50 μg/ml) for different times. (e, f) Western blotting analysis of LC3 (e) and p62 (f) levels in U-2OS cells after they were incubated with or without ZnO NPs (50 μg/ml) for 24 h after 2 h pre-treatment with CQ (10 μM). LC3 and p62 levels were detected by western blotting and quantified by densitometric analysis relative to β-actin. Statistically significant differences were evaluated using the paired Dunnett`s t-test or one-way ANOVA. Results were expressed as the mean ± S.D. from three independent experiments. *$P<0.05$ versus control, $^{\#}P<0.05$ versus ZnO NPs treatment.

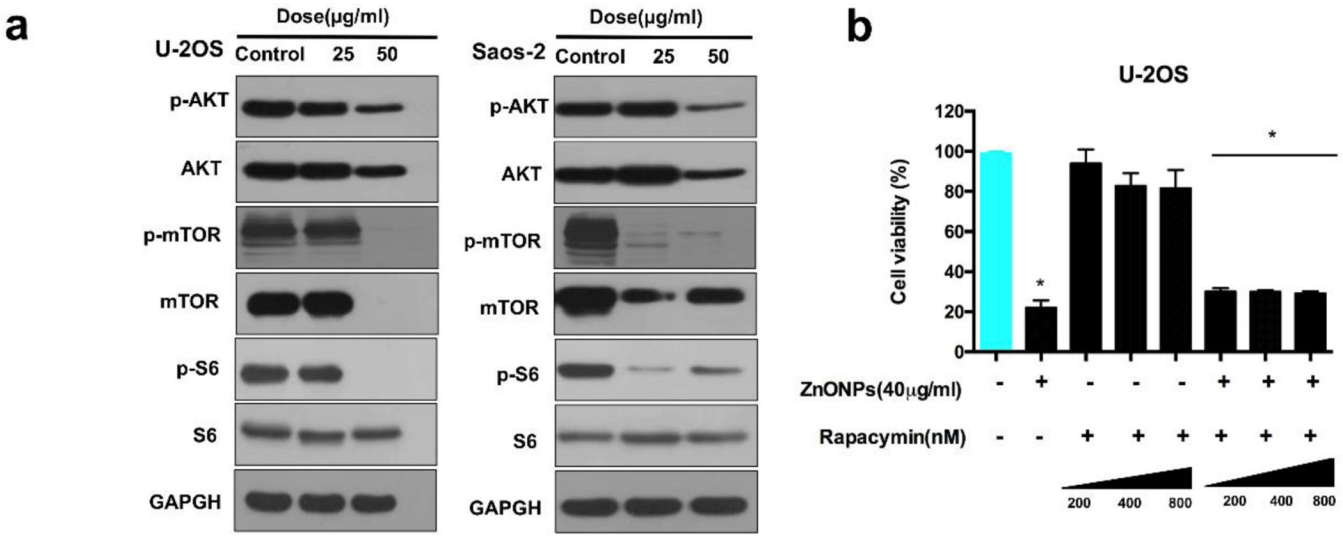

Figure 5.

Effect of ZnO NPs on the Akt/mTOR signaling pathway. (a) Western blotting analysis of the expression of mTOR/p-mTOR, Akt/p-Akt and S6/p-S6 in the U-2OS cells after they were treated with ZnO NPs for 24 h. (b) CCK-8 analysis of U-2OS cells after they were pretreated with rapamycin for 2 h and exposed to ZnO NPs (40μg/ml) for 24 h. Statistically significant differences were evaluated using the paired Dunnett`s t-test or one-way ANOVA. Results were expressed as the mean ± S.D. from three independent experiments. *P<0.05 versus control.

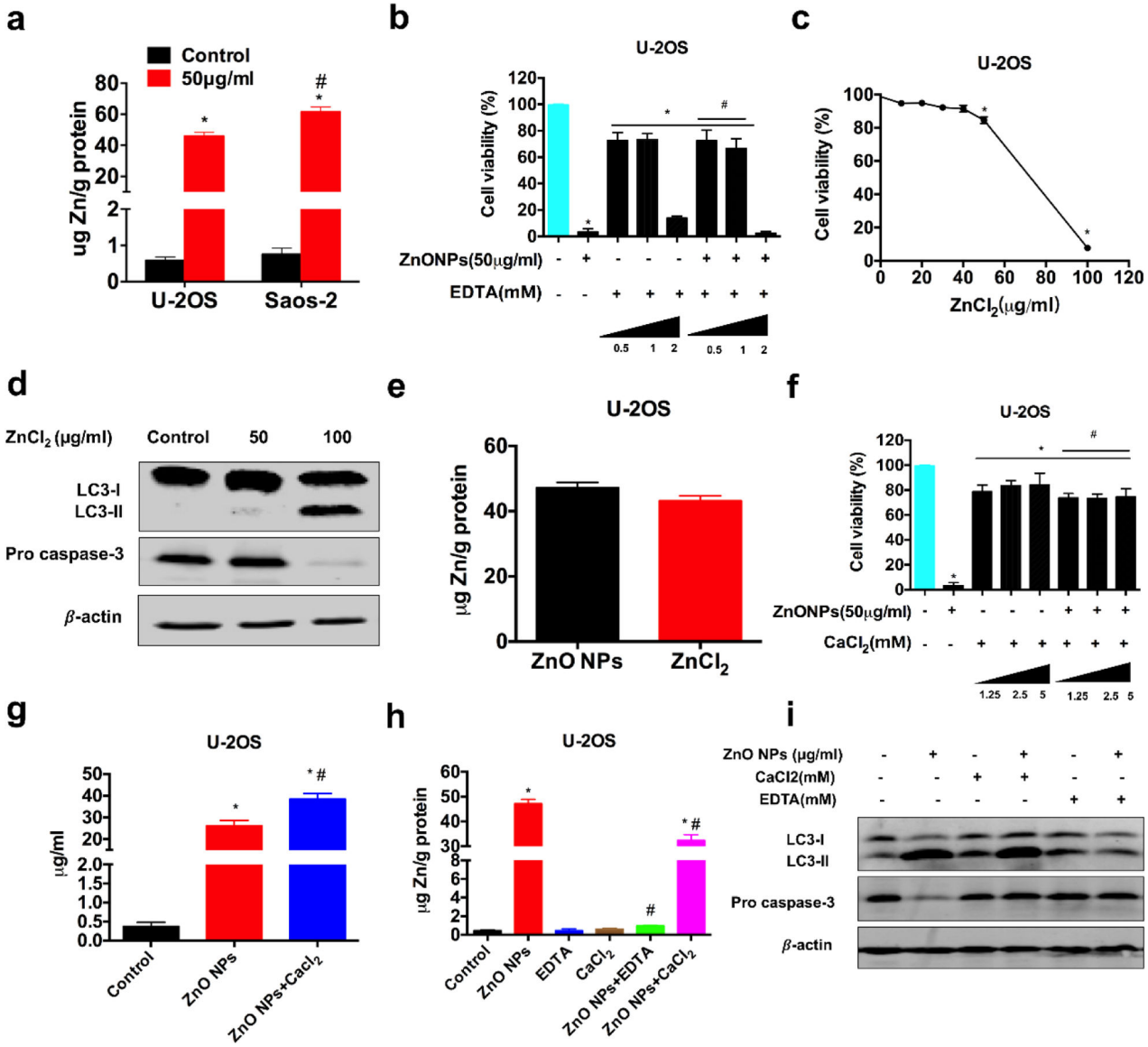

Figure 6.

The role of zinc ions in ZnO NPs-induced osteosarcoma cell death. U-2OS cells were pre-incubated with EDTA or $CaCl_2$ for 1 h, and then treated with ZnO NPs (50 μg/ml) for 24 h. (a) The concentration of intracellular zinc ions detected by ICP-MS for U-2OS and Saos-2. (b, f) Cell viability analyzed by CCK-8 in the presence and absence of EDTA (b) or $CaCl_2$ (f) with varying concentrations. (c, d) Cell viability analyzed by CCK-8 (c) and LC3 and pro caspase-3 levels detected by western blotting (d) after the cells were exposed to varying concentrations of $ZnCl_2$. (e) The concentration of intracellular zinc ions after the osteosarcoma cells were under the equivalent inhibitory effect of ZnO NPs and $ZnCl_2$. (g) The concentration of zinc ions in the supernatant released from ZnO NPs with or without $CaCl_2$ detected by ICP-MS. (h) The concentration of intracellular zinc ions detected by ICP-MS in the presence and absence of EDTA or $CaCl_2$. (i) LC3 and pro caspase-3 levels was detected by western blotting in the presence and absence of EDTA or $CaCl_2$. Statistically

significant differences were evaluated using the paired Dunnett`s t-test or one-way ANOVA. Results were expressed as the mean ± S.D. from three independent experiments. *P<0.05 versus control, #P<0.05 versus ZnO NPs treatment.

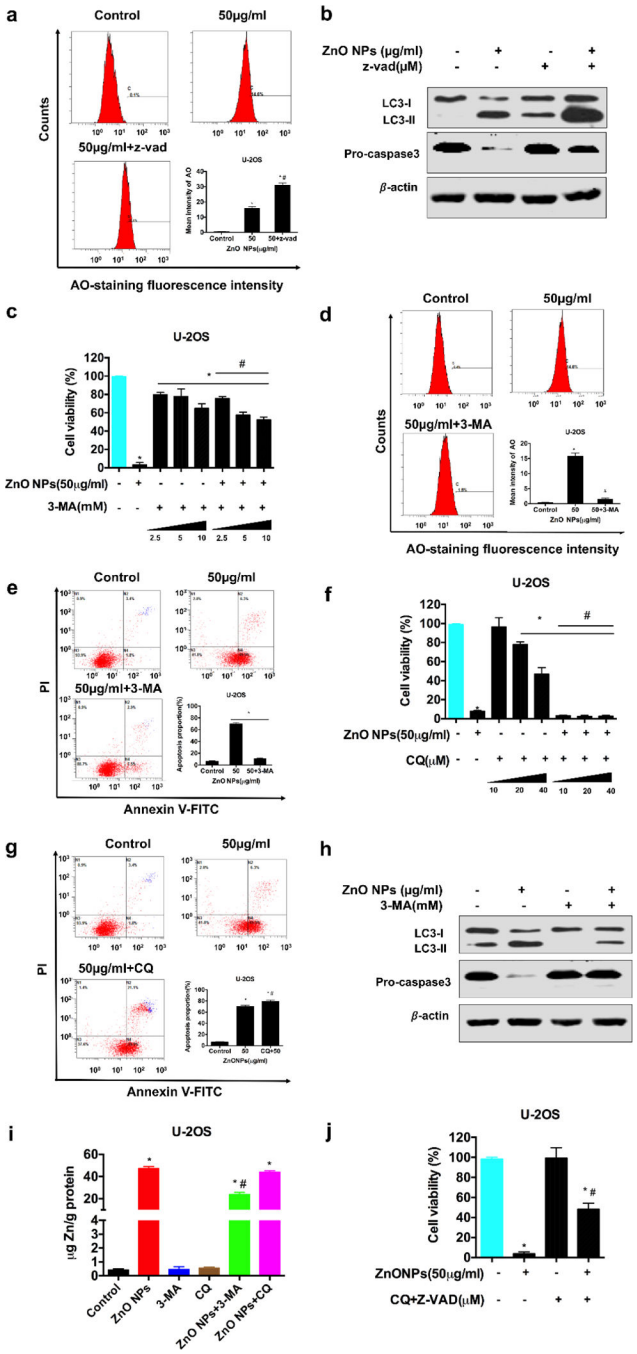

Figure 7.

Crosstalk between apoptosis and autophagy. U-2OS cells were pre-incubated with z-vad-fmk, 3-MA or CQ for 2 h, and then treated with ZnO NPs for 24 h. (a, b) The levels of AO staining determined by flow cytometry (a) and the levels of LC3 and pro caspase-3 detected by western blotting in the presence and absence of z-vad-fmk (20 μM) (b). (c, d, e, h) Cell viability detected by CCK-8 in the presence and absence of 3-MA with varying concentrations (c), apoptotic proportion analyzed by flow cytometry with AO-staining (d) and annexin V-FITC/PI staining (e) and LC3 and pro caspase-3 levels detected by western

blotting (h) in the presence and absence of 3-MA (10 nM). (f, g) Cell ability detected by CCK-8 in the presence and absence of CQ with varying concentrations (f) as well as apoptotic proportion analyzed by flow cytometry with annexin V-FITC/PI staining in the presence and absence of CQ (10 μM). (i) The concentration of intracellular zinc ions in the presence and absence of 3-MA (10 nM) and CQ (20 μM). (j) Cell viability detected by CCK-8 in the presence and absence of CQ (10 μM) and z-vad-fmk (20 μM). Statistically significant differences were evaluated using the paired Dunnett`s t-test or one-way ANOVA. Results were expressed as the mean ± S.D. from three independent experiments. *$P<0.05$ versus control, $^{\#}P<0.05$ versus ZnO NPs treatment.

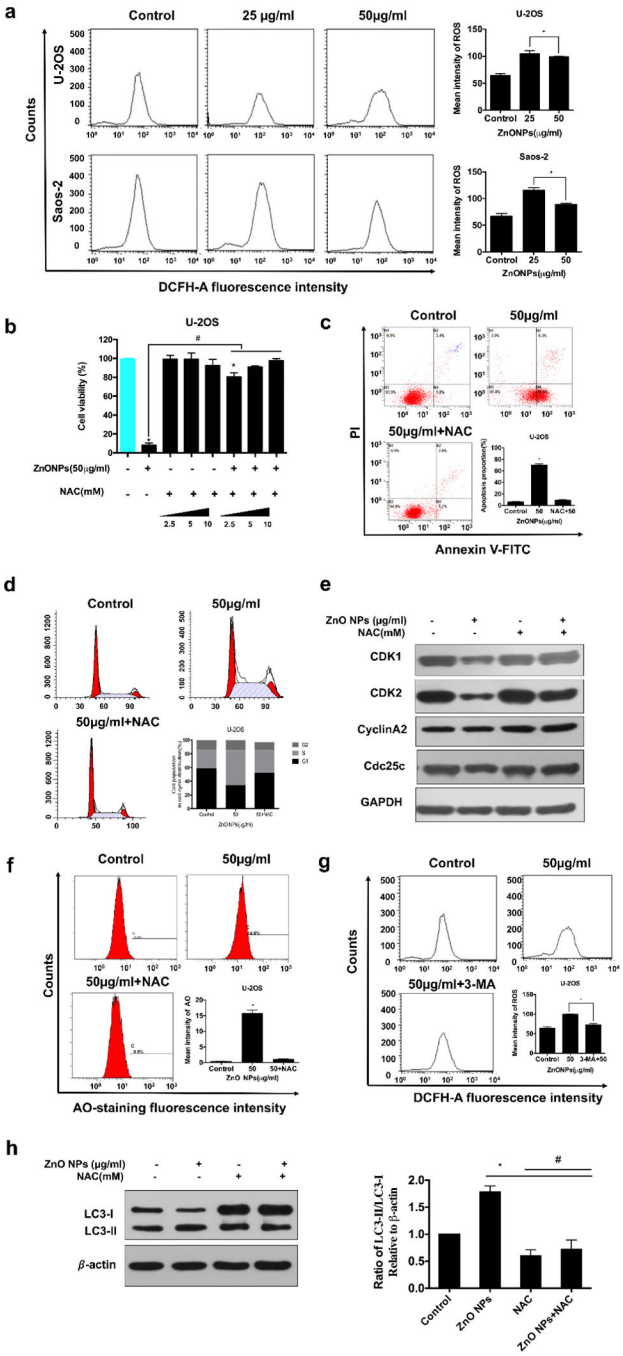

Figure 8.

The role of ROS in ZnO-induced osteosarcoma cell death. U-2OS cells were pre-incubated with NAC (10 nM) for 1 h, 3-MA (10 nM) for 2 h and then treated with ZnO NPs (50 μg/ml) for 24 h. (a) Cells were loaded with DCFH-DA and then the levels of ROS were analyzed by flow cytometry. (b, c, d, e) Cell viability detected by CCK-8 in the presence and absence of NAC with varying concentrations (b), apoptosis (c) and cell cycle (d) analyzed by flow cytometry in the presence and absence of NAC, and cell cycle related proteins detected by western blotting (e). (f) The levels of AO staining in the presence and absence of NAC

analyzed by flow cytometry. (g) LC3 levels detected by western blotting and quantified by densitometric analysis relative to β-actin. (h) The levels of ROS analyzed by flow cytometry after the cells were labeled with DCFH-DA for 30 min. Statistically significant differences were evaluated using the paired Dunnett`s t-test or one-way ANOVA. Results were expressed as the mean ± S.D. from three independent experiments. *P<0.05 versus control, #P<0.05 versus ZnO NPs treatment.

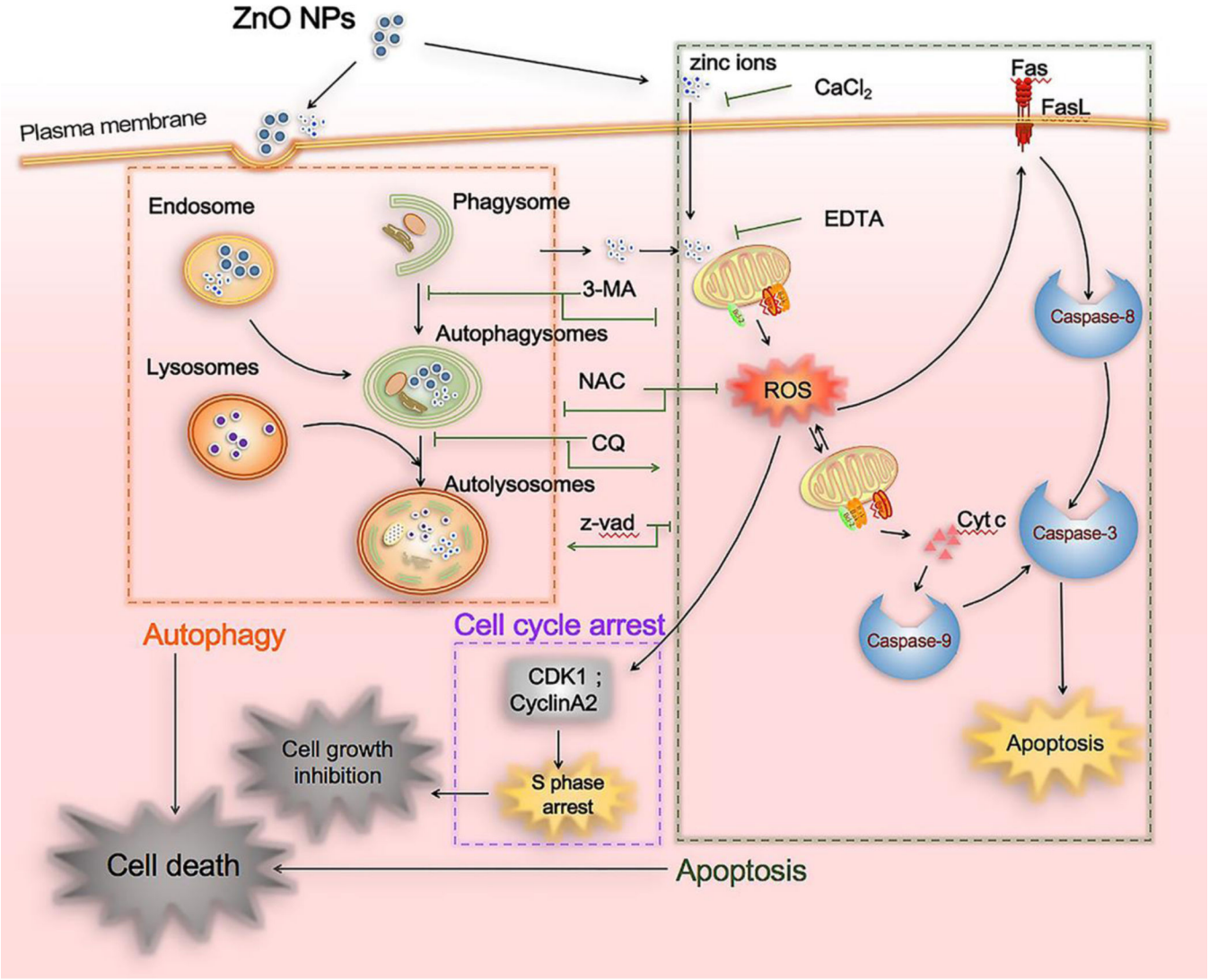

Figure 9.

Overview of the ZnO NPs induced cell death pathways. ZnO NPs can induce accumulation of autophagosomes and impair lysosomal functions. Moreover, ZnO NPs can utilize autophagy to enhance zinc ions release through promoting the dissolution of ZnO NPs. The released zinc ions, together with the intracellular zinc ions arising from the inflow of the extracellularly released zinc ions (from the extracellular ZnO NPs), collectively target and damage mitochondrion, resulting in the generation of ROS. The ROS then inhibits cell proliferation by S phase arrest and induce cell apoptosis through the extrinsic (Fas, caspase-8) and intrinsic (bax, bcl-2, caspase9) pathways, ultimately leading to cell death. Elimination of ROS with NAC can completely reverse the cell viability. Inhibiting the early stage autophagy with 3-MA abolishes the apoptosis while inhibiting the late stage autophagy with CQ inversely promotes the apoptosis. In contrast, suppressing apoptosis with z-vad-fmk fails to rescue cell death but enhances autophagy.